ACS EARTH AND SPACE CHEMISTRY

http://pubs.acs.org/journal/aesccq

Article

Organic Adsorption onto Iron Hydroxide and Sulfide Minerals: Implications for Ceres Sample Return Analysis

Eduardo Martinez, Erika Flores, Dennise Valadez, Jessica M. Weber,* David VanderVelde, Rachel Y. Sheppard, Robert Hodyss, Julie Castillo-Rogez, Mohit Melwani Daswani, Bryana L. Henderson, and Laura M. Barge*

Cite This: https://doi.org/10.1021/acsearthspacechem.4c00372

Read Online

ACCESS | Metrics & More | Article Recommendations | Supporting Information

ABSTRACT: Characterizing the past and present habitability potential of Ceres is an important goal of a future NASA mission to the dwarf planet. Signs of organic molecules (potentially amino acids, carboxylic acids, etc.) and their potential interactions with surrounding minerals may be present on the surface of Ceres. In addition, iron minerals are postulated to be present based on Dawn's gamma ray and neutron detector measurements, and iron minerals are known to be able to adsorb organic molecules. To understand if these iron minerals could adsorb prebiotically relevant organics on the surface of Ceres, we conducted an experimental study to test the adsorption of a set of simple organics (alanine, glycine, acetate, malic acid, and aspartic acid) on two classes of iron minerals found in carbonaceous chondrites (Fe-sulfides and Fe-hydroxides, synthesized via coprecipitation). Our experiments revealed little to no adsorption of amino acids onto each of the Fe-minerals. Our results also revealed that the redox state of the Fe-hydroxide minerals remained stable throughout the experiment; however, Fe-sulfide precipitates exhibited reduction of Fe(III) to Fe(II). Additionally, there was negligible adsorption of glycine onto mixed-valent iron mineral systems in a synthetic brine solution. This work shows that organic acids remain stable in the presence of Fe-bearing minerals and are mobile when dried and rehydrated by brines, meaning that these organics may be stable on Ceres' surface but could be further mobilized during cryovolcanic events, the products of which may be used for further reactivity toward other complex molecules with astrobiological relevance.

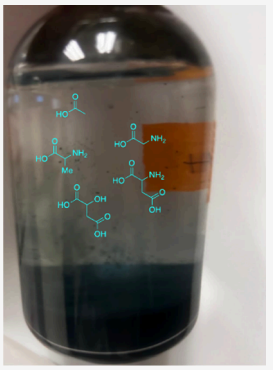

KEYWORDS: *Ceres, organic adsorption, iron sulfides, iron (Hydr)oxides, amino acids, habitability*

INTRODUCTION

Ceres, a dwarf planet located within the asteroid belt, has become a prime target of astrobiological significance, especially because its abundant water-ice content, geochemically rich past, and presence of organic compounds suggest that it could have been habitable in the past and possibly at present.[1−5] The 2023−2032 Planetary Science and Astrobiology decadal survey has included a sample return mission to Ceres as a part of the New Frontiers mission portfolio.[6] That mission would address (1) Ceres' current habitability potential and its contribution to studying the habitability of icy worlds; (2) identify Ceres' origins; and (3) quantify the evolution of organic compounds in a long-lived brine reservoir, with implications for understanding other inner solar system planetary bodies.[4−8] Observations by Dawn's visible and infrared mapping spectrometers (VIR) reveal the presence of Mg/Al phyllosilicates, ammoniated phyllosilicates, carbonates, and Fe-bearing minerals (magnetite and Fe-sulfides) believed to be from aqueous alteration.[5,7,9,10] Additionally, modeling efforts revealed that the darkening agents found on Ceres' surface are likely to be magnetite and/or Fe sulfide minerals with amorphous organics, which are consistent with the data obtained from the Dawn gamma ray and neutron detector (GRaND).[11,12] Dawn also revealed the presence of aliphatic organics at Ernutet crater (based on the 3.4 μm band detected by VIR) similar to those found on carbonaceous chondrite meteorites and likely endogenously sourced.[1,13,14] As one of the largest icy planetesimals, Ceres' evolution as a result of water-rock alteration may help us to understand prebiotic chemistry in bodies that contributed water and organics to the inner solar system.[5]

Iron minerals are highly reactive and can be easily oxidized or reduced by their surrounding environmental conditions as well as by organic reagents.[15,16] Iron minerals have a range of oxidation states, each state with unique structural and reactive properties that can influence the fate of organic molecules and can shield organics from photochemical and biological oxidation/degradation.[17−19] Ceres' inferred alkaline conditions[20] could enable the precipitation of reactive Fe-hydroxides and Fe-sulfides that could also react with organic molecules.

Received: December 3, 2024
Revised: April 7, 2025
Accepted: April 8, 2025

Mineral surfaces can serve as a binding site for organic or inorganic compounds to adhere to the mineral surface via different adsorption mechanisms (e.g., ligand exchange, H-bonding, Lewis acid−base interactions, etc.).[16,21,22]

To understand the complex chemistry that may have occurred on the surface of Ceres to contextualize its potential habitability, it is important to characterize the interactions between precipitated Fe minerals and a potential organic material. The characterization of the organic material on Ceres is currently limited to information from the structure of the 3.4 μm VIR band that indicates the presence of methyl (CH_3) and methylene (CH_2) functional groups.[23,24] The abiotic synthesis of organic molecules (such as amino acids and α-hydroxy acids) on planetary bodies is of particular interest given that they are critical to life as we know it, for example, amino acids are necessary for protein generation,[25] while α-hydroxy acids are key intermediates in the tricarboxylic acid cycle which is found in many organisms.[26,27] Like carbonaceous chondrites (CC chondrites), Ceres could have locales for abiotic amino and α-hydroxy acid synthesis via mechanisms such as Strecker synthesis, reductive amination, and aldehyde plus ammonia reactions.[28−30] Given that Ceres has reactive minerals as well as organic molecules to drive organic acid synthesis, we investigated if organic acid adsorption occurs onto minerals found on Ceres once they have been synthesized.

Here, we tested several Fe-hydroxide and Fe-sulfide mineral types, which are known to transform into magnetite (and other iron oxides), making them relevant to the GRaND measurements.[31,32] We investigated the effect of the redox state of the iron mineral on the adsorption of five organic molecules (alanine, glycine, acetate, malic acid, and aspartic acid) of prebiotic relevance and have been shown to be synthesized abiotically.[28−30] In fact, reactions with iron minerals have been demonstrated to produce abiotic amino acids, α-hydroxy acids, and others via iron minerals, including Fe-hydroxides and Fe-sulfides in our group and by other investigators.[29,33−35] We also investigated whether these organics are mobile if the mineral/organic mixture is desiccated and rehydrated with brine, such as what might occur in successive brine flows in cryovolcanic sites on Ceres.

MATERIALS AND METHODS

All experiments were performed at room temperature in a nitrogen-filled glovebox. No adjustment was made to the temperature, as we were focused on exploring the mineral−organic interaction. Future work could explore varying the temperature. All solutions were prepared with deionized Milli-Q water (18.2 MΩ•cm) that had been sparged with N_2 (30 min per 100 mL H_2O). In order to explore these reactions, the iron minerals were synthesized within the lab based on previously published literature.[17,33] Iron solutions for mineral precipitation were prepared using $FeCl_2$•$4H_2O$ and/or $FeCl_3$•$7H_2O$ (Fisher Scientific), sulfide solutions were prepared using Na_2S•$9H_2O$ (Sigma-Aldrich), and organic acid solutions were prepared using the following: L-alanine (99% pure, Thermo Scientific), glycine (98% pure, Acros Organics), sodium acetate (99% pure, Fisher Chemical), DL-malic acid (99−100.5% pure, VWR), and aspartic acid (99% pure, Sigma). The organics were used without any additional purification. Titrating solutions were prepared by using NaOH (Avantor) and HCl (Sigma-Aldrich).

Organic Acid Adsorption Experiments in Aqueous Solution. In our experiments, we refer to adsorption as the surface interaction between our Fe minerals and organic acids, primarily because our minerals can undergo Lewis acid−base interactions rather than absorption, given the lack of a layered structure (e.g., clay minerals) in our minerals. The sorption of organics (alanine, glycine, acetate, malic acid, aspartic acid) onto lab-synthesized Fe-hydroxide and Fe-sulfide minerals was tested at pH 10 (Table SI-1). The organic acid adsorption experiments were performed at 25 °C and at standard atmospheric pressure (1 atm) to understand adsorption under stable conditions and minimize the introduction of additional variables. This method allowed us to isolate the effects of adsorption on a stable temperature and also assess the influence of temperature on our Ceres brine freeze-dried experiments (described below). A 140 mL stock solution of Fe-hydroxide was prepared by precipitating 131.25 mL of dissolved $FeCl_2$•$4H_2O$ and/or $FeCl_3$•$7H_2O$ with 8.75 mL of 1 M NaOH. A 160 mL stock solution of FeS was prepared by combining 80 mL of dissolved $FeCl_2$•$4H_2O$ and/or $FeCl_3$•$7H_2O$ with 80 mL of Na_2S•$9H_2O$. Twenty-five mM organic stock solutions were prepared and titrated to pH 10 with NaOH or Na_2S. For each experiment, 20 mL of precipitated mineral slurry and 5 mL of organic stock solution were combined to make a solution with a final Fe concentration of 50 mM, NaOH or Na_2S•$9H_2O$, and 5 mM organic stock solution while being continuously stirred. For experiments using Fe-hydroxides, pH values of the organic and the Fe mixtures were below 10; therefore, additional NaOH was added to reach a pH value of 10. High pH was needed to create the mineral; however, this is relevant to possible water-rock interactions on Ceres. Processes such as serpentinization could be a source of magnetite, raise the pH of surrounding fluids (pH > 9), and create reducing conditions.[28,29] The pH prior to adjustment for experiments with 100% Fe^{2+} was ∼6−7, and experiments with 50% = Fe^{2+}:Fe^{3+} and 100% Fe^{3+} were ∼1.50 − 2.0. This solution was then titrated to pH 10 using aq. NaOH and aq. HCl. The effect of the mineral's redox state on organic sorption was tested by varying the Fe^{2+}:Fe^{3+} ratio. Three iron ratios (Fe^{2+} = 100%, Fe^{2+}:Fe^{3+} = 50%, and Fe^{3+} = 100%) were tested for each type of mineral. Each experiment was placed in a stir plate and was constantly stirred for 2 weeks at 100 rpm. Each experiment was performed four times. A full list of experiments (Table SI-1) and images of the experimental serum vials (Figures SI-1 and SI-2) can be found in the Supporting Information. Six 1 mL aliquots were taken from each mineral/organic solution at t = 0 (after titrating to pH 10), 1 week, and 2 weeks. The pH of the experiments was measured using a Thermo Scientific Orion Star A211 Benchtop pH meter at each sampling time point (Figure SI-23). The liquid phase was analyzed with ^{1}H NMR to determine organic concentration, and the solid material was analyzed with iron colorimetry to determine Fe redox state. At the end of each experiment, the remaining solution and minerals were removed from the stir plate and left to settle inside the glovebox to prevent atmospheric oxidation of our Fe minerals. The supernatant was then pipetted out, and the bottle was covered with parafilm and transferred to an SP Scientific Virtis AdVantage benchtop freeze-dryer to freeze-dry over 3 days. The benchtop freeze-dryer was not equipped with an inert gas supply. All experiments were removed from the glovebox and were exposed to atmospheric oxidation during the freeze-dry processes, which may have altered the redox state of the minerals at the end of the experiment. Once dry,

https://doi.org/10.1021/acsearthspacechem.4c00372
ACS Earth Space Chem. XXXX, XXX, XXX−XXX

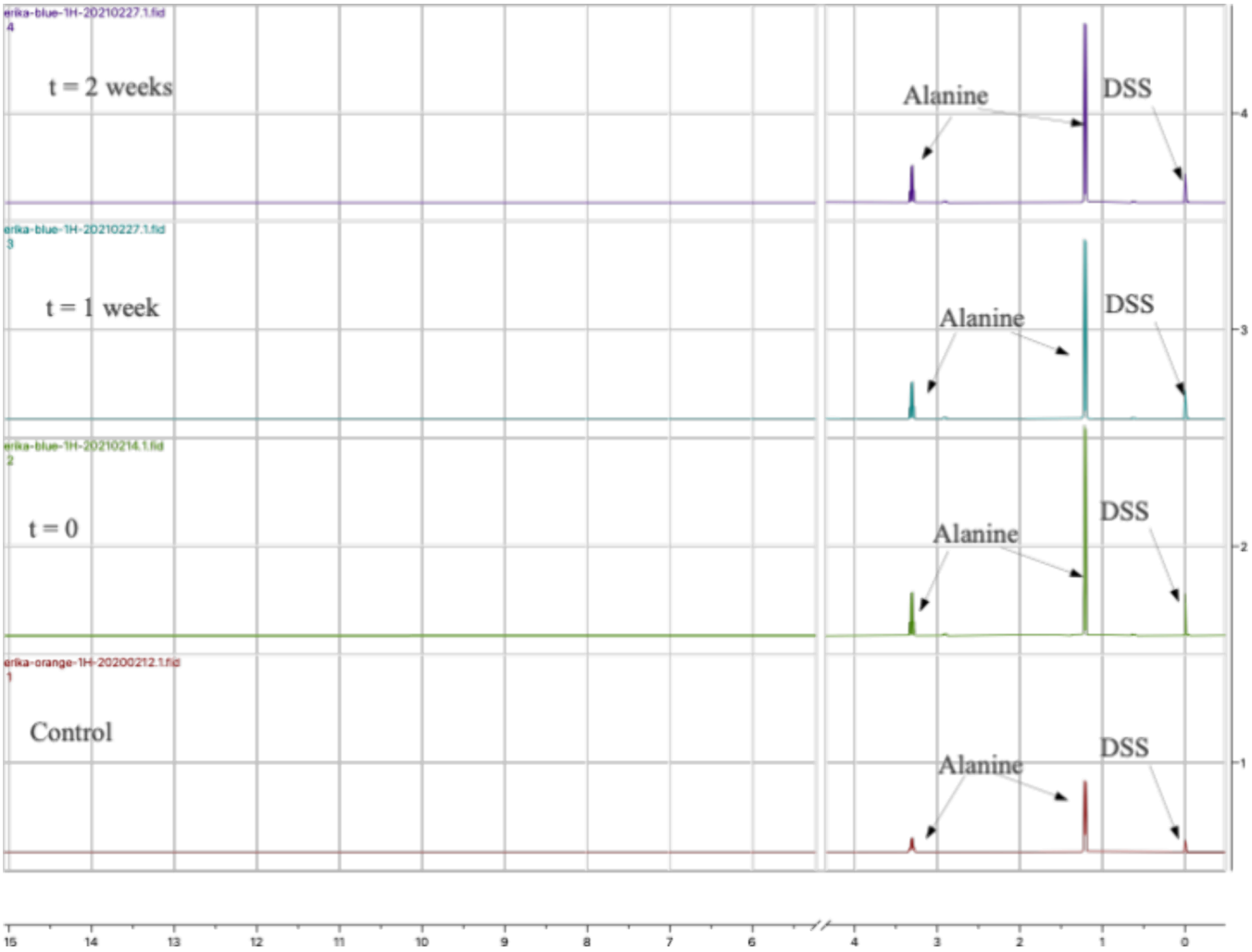

Figure 1. NMR spectra of alanine peaks from experiment containing Fe(II)-hydroxide at pH 10. The water peak is omitted for the sake of clarity.

the samples were transferred to microcentrifuge tubes and stored in the glovebox until ready for further analysis.

Ceres Brine Rehydration Experiments. To estimate the composition of a Ceres brine (representing eruption from near surface brine reservoirs onto the surface), we modeled in Geochemist's Workbench a brine composition for a pH of 6.5 and water/rock ratio of 10. The GWB output (Table SI-9) derived the molal concentration of major aqueous species in a brine; we chose to include in our estimates those species that were present at concentrations above 0.001 molal (these included HCO_3, NH_4^+, Na^+, Cl^-, Ni_2^+, $NaHCO_3(aq)$, $MgHCO_3^+$, Mg_2^+, and K^+). We derived a recipe for a laboratory Ceres brine solution (Table SI-9) including salts of these species to approximate the concentrations from Table SI-8. The Ceres brine analogue solution was composed of 7.86 $\times$ 10^{-2} M $(NH_4)_2CO_3$ (Sigma-Aldrich), 1.66 $\times$ 10^{-2} M $NaHCO_3$ (Fisher Scientific), 1.91 $\times$ 10^{-2} M NH_4Cl (Fisher Scientific), 6.80 $\times$ 10^{-3} M $MgCl_2{\cdot}6H_2O$ (Fisher Scientific), 1.71 $\times$ 10^{-2} M $NiCl_2$ (Sigma-Aldrich), 6.88 $\times$ 10^{-3} M $MgCO_3$ (Sigma-Aldrich), and 2.21 $\times$ 10^{-3} M KCl (Mallinckrodt); titrated to pH 6.5. Stock solutions of Fe-hydroxide and Fe-sulfide minerals for the Ceres brine experiments were prepared in the same manner as that stated in the aqueous organic acid adsorption experiments. For these brine experiments, however, only one redox state (50% = Fe^{2+}:Fe^{3+}) and only one organic molecule (glycine) were tested.

Control experiments of Fe-hydroxide (50% = Fe^{2+}:Fe^{3+} and NaOH) and Fe-sulfide (50% = Fe^{2+}:Fe^{3+} and Na_2S) were performed by precipitating 50 mL of each mineral without the addition of any organics and freeze-dried without the removal of any supernatant. A thermocouple was inserted into each bottle to monitor the conditions of the mineral throughout the freezing/drying process. A Kimwipe was used to cover the thermocouple and avoid cross-contamination between experiments. A freeze-dryer recipe was developed to ensure that the samples would dry in a period of 3 days. A detailed description of the freeze-drying process is provided in the SI, involving only one freezing cycle followed by drying. Once dry, the minerals were removed and brought into the glovebox, where they were rehydrated with 50 mL of the Ceres brine solution. Mineral/brine solutions were placed on a stir plate at 100 rpm for 2 weeks, with sampling in between. Six 1 mL aliquots were taken prior to freeze-drying, upon addition of the Ceres brine solution (t = 0), and at 1 and 2 weeks of stirring post Ceres brine solution addition. These samples were frozen to preserve them for later analysis with nuclear magnetic resonance (NMR) and iron colorimetry. These experiments were then repeated but with the addition of glycine, which was weighed

https://doi.org/10.1021/acsearthspacechem.4c00372
ACS Earth Space Chem. XXXX, XXX, XXX−XXX

out and added directly to the mineral before freeze-drying. All experiments were repeated three times.

Analytical Techniques. ^{1}H Nuclear Magnetic Resonance (NMR) Spectroscopy. Prep for NMR analysis involved centrifuging three of the samples, transferring 0.75 mL of supernatant to a new microcentrifuge tube with 0.25 mL of 1 M NaOH to precipitate out any soluble Fe, and centrifuging again. The supernatant was then used to prepare NMR samples by taking 0.54 mL from the microcentrifuge tube and adding 60 μL of DSS in D_2O (sodium trimethylsilylpropanesulfonate/deuterium oxide) as standard to an NMR tube. ^{1}H NMR spectra were acquired on a 400 MHz Bruker spectrometer equipped with an auto sampler. The spectra were processed with the MestReNova NMR analysis software. The concentrations (mM) of each organic in the mineral supernatant were also calculated by using the NMR methyl peak areas in comparison to the DSS peak (which was integrated to 1). The NMR spectra can be found in the SI for each experiment. The average percent change was calculated by using the following equation, percent increase or decrease (%) = $(t_0 - t_x)/t_0$ where t_0 is the concentration of organic detected in the supernatant at $t = 0$ and t_x is the concentration detected in the supernatant of samples taken at either $t = 1$ week or $t = 2$ weeks. Sample $t = 0$ is the time point at which the organic acids were added to the experiment and processed for NMR (within 10 min).

Fe^{2+} Colorimetry. To track the oxidation state of iron, 1 mL of 10 M HCl was added to three liquid−solid samples that were then heated at 100 °C for a few minutes to dissolve the mineral precipitate. Once fully dissolved, the samples were diluted and run in a Thermo Fisher GENESYS 30 Visible spectrophotometer set to a wavelength of 510 nm using a slightly modified version of a Fe^{2+} colorimetry technique.[36] The % of Fe^{2+} in the dissolved samples was calculated, and the averages from all repeats are plotted. The ratio of Fe^{2+}/Fe(T) was used to report the percent of Fe(II) in our experiments, where FeT (Fe Total) is equal to the sum of the Fe^{2+} and Fe^{3+}.

Visible Near-Infrared (VNIR) Reflectance Spectroscopy. The spectral reflectance of lyophilized mineral samples at 2 weeks was obtained by an analytical spectral device (ASD) FieldSpec3 spectroradiometer with a wavelength range of 0.3−2.5 μm and a resolution of 3 (350−1000 nm) or 10 nm (1000−2500 nm). Sample spectra were collected against a Spectralon white reference (Figure 1). The dried mineral samples were placed on either white weighing paper (VWR) or black Cinefoil and illuminated by a fiber optic cable with a while light source (quartz tungsten halogen) on a hand-held contact probe. The powdered samples were pressed against the contact probe, and the spectral reflectance was collected on RS.[3] In between samples, the probe was wiped with a Kimwipe. The samples were collected and saved post VNIR analysis.

■ RESULTS AND DISCUSSION

Organic Acid Adsorption onto Fe (Oxy)hydroxides. In Fe-hydroxide experiments, we observed similar trends of the organic acids' (Table 1) adsorption onto each of the Fe-hydroxide mineral conditions. In experiments containing 100% Fe(II)-hydroxide minerals, adsorption of all organic compounds tested increased to approximately <16% at $t = 2$ weeks. The two most adsorbed organic acids in the Fe(II)-hydroxide experiments were malic acid and aspartic acid, with each adsorbing 14.25% and 15.85%, respectively (Figure 2A). In experiments with 50% = Fe(II)/Fe(III)-hydroxide the percent adsorbed remained relatively constant near ∼0% adsorbed at 1 and 2 weeks (Figure 2B). In experiments with 100% Fe(III)-hydroxide, all of the organic acids desorbed at 1 week and were later readsorbed except alanine and glycine (Figure 2C).

Table 1. Functional Groups and Properties of Organics Considered in This Work

organic	functional Group	pK_a	reference
alanine	carboxyl (COOH), amine (NH_2)	pK_1 = 2.3, pK_2 = 9.8	37
glycine	carboxyl (COOH), amine (NH_2), H atom	pK_1 = 2.3, pK_2 = 9.6	38
acetate	carboxyl (COOH), ester	pK_a = 4.76	39
malic acid	dicarboxyl (COOH)	pK_1 = 3.4, pK_2 = 5.2	40
aspartic acid	carboxyl (COOH), amine (NH_2)	pK_{a1} = 2.0, pK_{a2} = 3.9, pK_{a3} = 9.9	41

The pH decreased for experiments beginning with 100% Fe(II) and with 50% = Fe(II)/Fe(III), while the pH increased for experiments beginning with 100% Fe(III) (Figure SI-23). The decrease in pH followed the same trend for each mineral type; for example, in experiments with 100% Fe(II)-hydroxide precipitates, there was a decrease at $t = 1$ week and a slight increase at $t = 2$ weeks. The pH of the experiment between Fe(III)-hydroxides and the presence of alanine and glycine in solution remained stable at a pH level of 9.5, whereas all other organic molecules experienced lower pH's throughout the course of the experiment. The 50% = Fe(II)/Fe(III)-hydroxide experiments experienced a similar trend, where the experiments decreased from a pH of 10 to below 9.0 (Figure SI-23). Lastly, the pH of the experiments with 100% Fe(III)-hydroxide increased, with some increasing to approximately ∼10.3 over the 2 week time. The colorimetry results revealed that the redox of Fe hydroxide minerals remained stable throughout the experiments. The experiments beginning with 100% Fe(II)-hydroxide minerals remained reduced with the Fe^{2+}/FeT nearly at or near 100% (Figure 3A). In experiments beginning with 50% = Fe(II)/Fe(III)-hydroxides, the minerals remained near their original redox state at 50% Fe^{2+} and 50% Fe^{3+} (Figure 3B). Lastly, in the experiments beginning with 100% Fe(III)-hydroxides, the minerals remained oxidized with Fe^{2+}/FeT being less than 5% (Figure 3C).

Organic Acid Adsorption onto Fe Sulfide Minerals. In Fe-sulfide mineral experiments, we did not observe substantial organic acid adsorption. In 100% Fe(II)-sulfide experiments, a trend was observed with alanine, malic acid, and aspartic acid, where organic acid concentrations remained the same for $t = 0$ and $t = 1$ week and were later desorbed around 2 weeks (Figure 2D). For experiments with 100% Fe(II)-sulfide minerals, glycine showed the highest adsorption (∼19.15%) at 1 week, followed by desorption, for a total of 2.22% adsorbed at 2 weeks. All organic acids reacting with 100% Fe(II)-sulfides, except for glycine, showed less than 5% adsorption for 1 week and 2 weeks. In Fe-sulfide mineral experiments starting with 50% = Fe(II)/Fe(III), malic acid was the highest adsorbed organic compound at 1 week (∼8.16%) and adsorption increased to 10.61% at 2 weeks. In the 50% = Fe(II)/Fe(III)-sulfide experiments, less than 5.00% of alanine, acetate, and aspartic acid were adsorbed in 1 week, followed by adsorption increasing at 2 weeks for a total of 6.10, 15.00, and 12.34% being adsorbed, respectively. Lastly, the experiment with 50% = Fe(II)/Fe(III) and glycine showed no adsorption until 2 weeks, where 9.32% of glycine was adsorbed (Figure 2E). In experiments with 100% Fe(III)-hydroxides reacting

https://doi.org/10.1021/acsearthspacechem.4c00372
ACS Earth Space Chem. XXXX, XXX, XXX−XXX

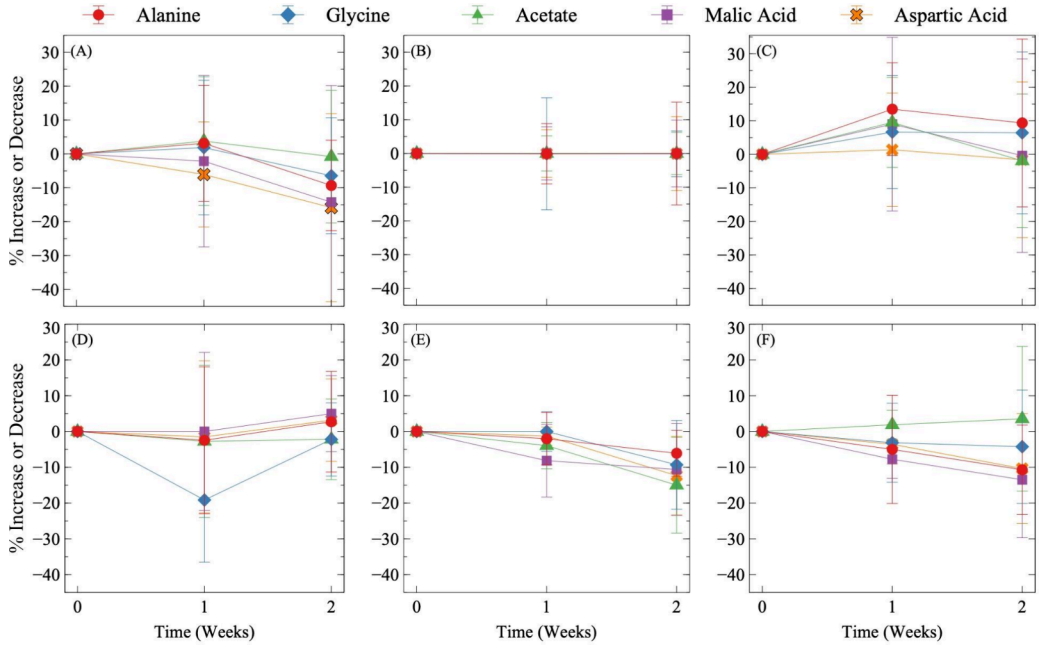

Figure 2. Average percent change of organic compounds in solution at t = 1 week and 2 weeks compared to t = 0 for both Fe (oxy)hydroxide (A–C) and Fe sulfide (D–F) minerals. Percent change greater than 0 (positive values) represents organics released from the mineral (a higher concentration of organic was detected in the supernatant). Percent less than 0 (negative values) represents the percentage of organics bound to the mineral increase at t = 1 week and t = 2 weeks compared to t = 0. (A) Experiments with 100% Fe^{2+} and NaOH, (B) experiments with 50% Fe^{2+}:Fe^{3+} and NaOH, (C) experiments with 100% Fe^{3+} and NaOH, (D) experiments with 100% Fe^{2+} and Na_2S, experiments with 50% Fe^{2+}:Fe^{3+} and Na_2S, and (F) experiments with 100% Fe^{3+} and Na_2S. The error bar represents the standard deviation from the average of experiments repeated four times.

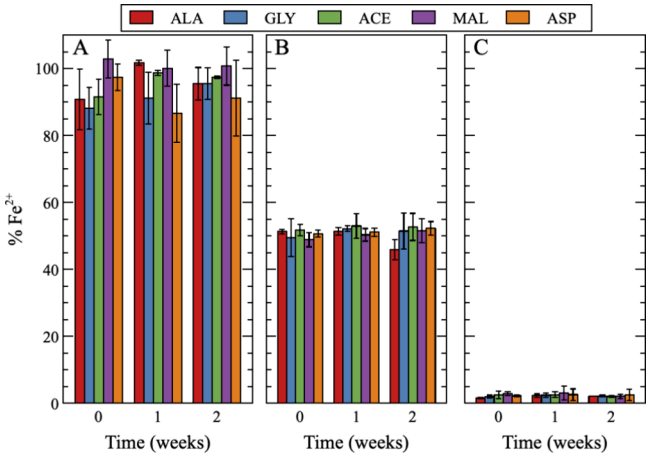

Figure 3. Fe oxidation state of Fe-hydroxide minerals reacted with the organic acids. (A) Experiments with Fe(II)-hydroxide and organic acids, (B) experiments with 50% = Fe(II)/Fe(III)-hydroxides reacting with organic acids, and (C) experiments 100% Fe(III)-hydroxide reacting with organic acids. The error bar is the standard deviation of the averages from all repeats.

with the organic molecules, minor adsorption was observed with alanine (5.01%), glycine (3.15%), malic acid (7.77%), and aspartic acid (3.59%) at 1 week and increased to 10.70, 4.26, 13.49, and 10.36% at 2 weeks, respectively (Figure 2E).

The Fe in the Fe-sulfide minerals was redox sensitive during the precipitation of our minerals. The precipitate formed for all starting Fe solutions was a black material despite the original oxidation state of the salt (i.e., $FeCl_2$ and $FeCl_3$). The colorimetry results of our Fe(II)-sulfide minerals show that the Fe remained as Fe(II) throughout the duration of the experiment (Figure 4A). In experiments with 50% = Fe(II)/Fe(III)-sulfide minerals, the partial Fe(III) in our minerals was reduced to Fe(II) during the initial sampling at t = 0 and remained reduced (>95.00% Fe^{2+}/FeT) for the 2 weeks (Figure 4B). The Fe(III)-hydroxides were also reduced during the start of the experiments (t = 0) and remained reduced (>95.00% Fe^{2+}/FeT) throughout the 2 weeks of the experiment (Figure 4C).

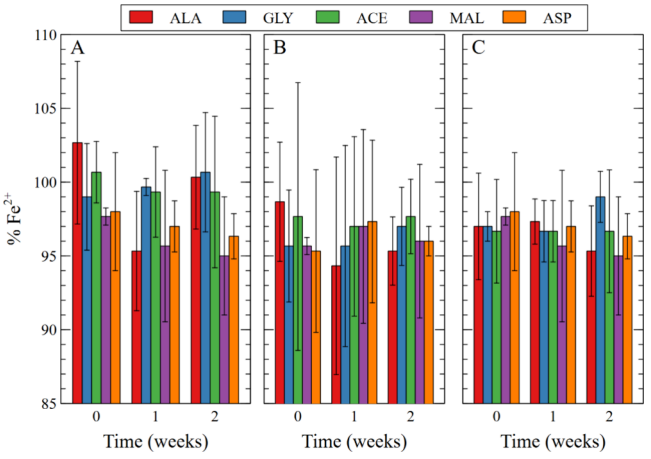

Figure 4. Fe oxidation state of Fe-sulfide minerals reacted with the organic acids. (A) Experiments with Fe(II)-sulfide and organic acids, (B) experiments with 50% = Fe(II)/Fe(III)-sulfide reacting with organic acids, and (C) experiments with 100% Fe(III)-sulfide reacting with organic acids. The error bar is the standard deviation of the averages from all repeats.

https://doi.org/10.1021/acsearthspacechem.4c00372
ACS Earth Space Chem. XXXX, XXX, XXX–XXX

Ceres Brine Solution Experiments. Adsorption of glycine was tested onto 50% = Fe(II)/Fe(III)-hydroxide and 50% = Fe(II)/Fe(III)-sulfide minerals. ^{1}H NMR was performed on the supernatant samples in solutions prior to freeze-drying, after freeze-drying, and rehydrating with the Ceres brine solution (t = 0), after constantly stirring that solution for 1 and 2 weeks. The spectra of the controls showed only the DSS/D_2O standard peaks and the glycine peak after it was added. For the Fe-50% = Fe(II)/Fe(III)-hydroxide and 50% = Fe(II)/Fe(III)-sulfide experiments without organic acids, there were no additional peaks detected. In the 50% = Fe(II)/Fe(III)-hydroxide, there was ∼6.00% adsorbed glycine and as later released at 2 weeks (Figure 5). In contrast, the

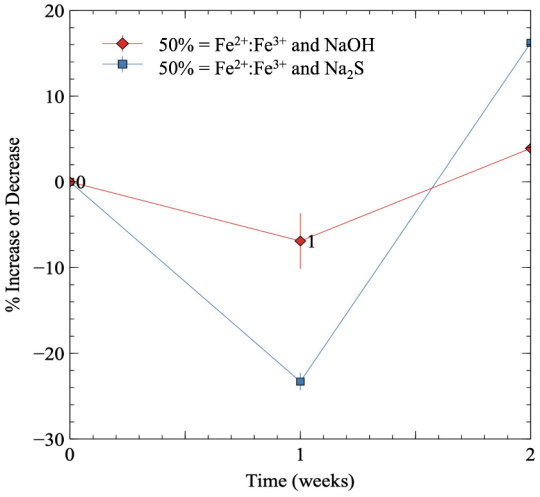

Figure 5. Average percent increase/decrease of glycine in 50% = Fe(II)/Fe(III)-hydroxide and 50% = Fe(II)/Fe(III)-sulfide minerals in a Ceres brine solution. Positive values represent organic molecules released from the mineral (a higher concentration of organic molecules detected in the supernatant). Negative values represent the percentage of organic molecules bound to the mineral increase at t = 1 week and t = 2 weeks compared to t = 0. The error bars are the standard deviation of the three experimental repeats.

50% = Fe(II)/Fe(III)-sulfide experiment showed that ∼20% of glycine was adsorbed to the mineral at 1 week and was later released at 2 weeks (Figure 5). Some differences between this work and the previous work could be attributed to mineral alterations (e.g., oxidation) in freeze-drying and other processing.

Reflectance spectroscopy. A range of overlapping electronic absorptions in the 0.35−2.5 μm wavelength range can be caused by the presence of ferrous and/or ferric Fe via intervalence charge transfer, oxygen−metal charge transfer, and crystal field splitting.[42−45] We observed two broad classes of mineral spectra. Our 100% Fe(II)-hydroxide minerals may be a chloride green rust, and it is important to note that the resulting oxidation was a result of atmospheric oxidation when the samples were removed from the glovebox for analysis. We have compared the reflectance spectra obtained from our experiments to the reflectance spectra of minerals in the RELAB VNIR library database.[46]

First, in Fe-hydroxide experiments with 100% Fe(II) (Figure 6A) and 100% Fe(III) (Figure 6C), there are strong electronic absorptions from 0.4 to 0.55 and 0.9 μm, consistent with abundant Fe oxides, possibly hematite (Figure 7). In the 100% Fe(II)-hydroxide experiments (Figure 6A), some samples (acetate and to a lesser extent alanine, glycine, and malic acid) exhibited hydration features at 1.9 μm associated with either structural or adsorbed water, suggesting the presence of another phase either with water in its mineral structure or a phase which is hygroscopic and adsorbs water to its surface easily. The hydration features are even stronger in the 100% Fe(III)-hydroxide experiments (Figure 6C), where all samples have 1.4 and 1.9 μm absorptions, indicating hydration of the sample. A small shoulder near 2.3 μm in the 100% Fe(III)-hydroxide experiments (Figure 6C) is a metal−OH vibration. The asymmetrical shape of the feature is more likely an Fe-oxide phase such as goethite, akageneite, butlerite, or ferrihydrite, which can also show small, asymmetrical absorptions in this area.[47,48] We note that the control in the 100% Fe(II)-hydroxide (Figure 6A) experiment is more consistent with magnetite, which may have undergone atmospheric oxidation while we transferred the samples to the freeze-dryer (see below).

Second, in Fe-hydroxide experiments with 50% = Fe^{2+}:Fe^{3+} (Figure 6B) and all Fe-sulfide experiments (Figure 6D−F), we see spectra broadly consistent with magnetite. Magnetite is a mixed valence iron oxide whose structure contains abundant octahedral Fe that leads to visible wavelength surface scattering and produces a spectrum that is broadly dark and flat with Fresnel peaks near 0.65 μm and a local reflectance minimum near 0.55 μm[49,50] (Figure 7). However, we note that Fe-sulfide experiments with 100% Fe(II) (Figure 6D) have minor hydration absorptions of ∼1.9 μm, reminiscent of the first group and possibly an intermediate case that has produced some amount of both magnetite and another hydrous phase. The slight oxidation from our fully reduced Fe-sulfide minerals, based on our colorimetry, may be a result of atmospheric oxidation similar which will lead to a magnetite, which is a stable mixed valent mineral under oxic conditions.

DISCUSSION

Organics present on Ceres are concentrated near Ernutet crater, where the spectral bands (3.3−3.5 μm) are prominent and are likely of endogenous origin.[1] In proposed analogue materials (CI, CM) to Ceres, organics (including amino acids) are a sizable part of the bulk composition.[23] In addition to organics, absorption bands have been interpreted as ammoniated clays[9] while other materials such as iron oxides (magnetite) and sulfides are predicted to be present, based on geochemical modeling.[12] Fe-hydroxide and Fe-sulfide minerals are known for their ability to adsorb organic molecules onto minerals.[51−54] Yet, for every organic molecule tested, we did not observe any condition in which a substantial amount of the organic acids were adsorbed. At alkaline pH, we would expect essentially all of the Fe in our experiments to be precipitated in the solid phase, and considering that the Fe:organic ratio was 10:1, there was a large excess of mineral compared to organics in these experiments. Therefore, an important finding from this work is that in all conditions tested, most of the organics remained in the aqueous phase, even in the presence of minerals and therefore mobile/available for reactivity. Over the 2 weeks of sampling, we did not observe the concentration of organics in the supernatant to change considerably (Figure 2). This means that the adsorption capabilities of a given mineral/organic combination are stable, at least in this experimental time frame.

Organic Acid Adsorption onto Fe (Oxy)hydroxides. Several factors can influence organic material adsorption on to

https://doi.org/10.1021/acsearthspacechem.4c00372
ACS Earth Space Chem. XXXX, XXX, XXX−XXX

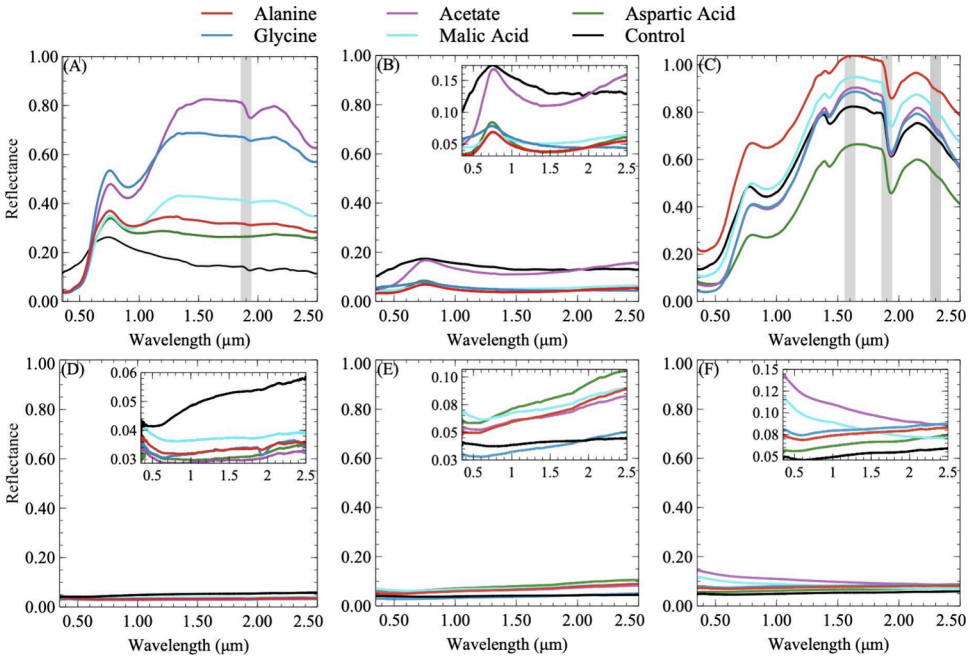

Figure 6. Spectral reflectance of Fe hydroxide and Fe-sulfide minerals reacted with and without organic acids. Reflectance spectra on the top show Fe-hydroxide experiments with and organic acids in experiments containing (A) 100% Fe(II)-hydroxides; the gray line at 1.9 μm indicates the hydration absorption feature (B) 50% = Fe(II)/Fe(III)-hydroxides (C) 100% Fe(III)-hydroxides; the gray lines at 1.6 and 1.9 μm indicate the hydration absorption feature, and the line at 2.3 μm indicates the metal−OH vibration. Reflectance spectra on the bottom show Fe-sulfide experiments containing (D) 100% Fe(II)-sulfides (E) 50% = Fe(II)/Fe(III)-sulfides and (F) 100% Fe(III)-sulfides.

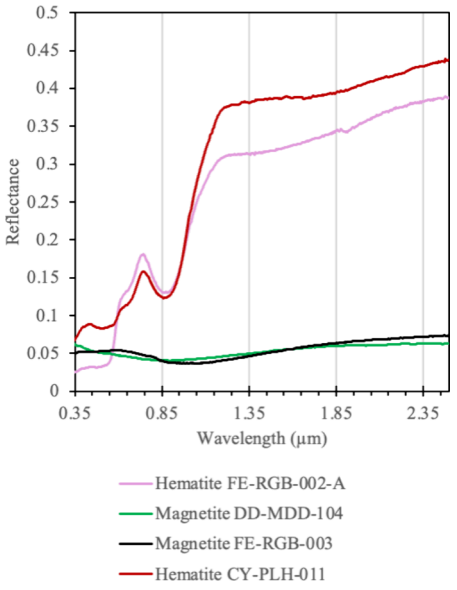

Figure 7. RELAB library VNIR reflectance spectra of hematite (pink, red) and magnetite (black, green)[42] for comparison.

Fe-hydroxide minerals, for example, particle size, structure of the mineral, solution composition, and type of adsorbate. An adsorption study of arginine onto mesoporous materials observed decreased adsorption as the ionic strength of the experimental solution increased in experiments at pH 10.[58] Gao et al. explain three ionic strength factors NaCl content can have on surface interactions: (1) the surface charge density of the material becomes more negative; (2) NaCl negatively affects the solubility of amino acids; (3) Na^+ ions can block negative charges on materials reducing adsorption capacity.[58] In studies using goethite (an Fe(III)-oxyhydroxide), oxalate, malonate, phthalate, lactate, and citrate adsorption decreased as pH increased.[59] Our experiments were initially titrated to pH 10, meaning the surface of our materials would be saturated with OH^- groups, and the introduction of NaOH into the solution might have influenced our experiments, as Gao et al. explained.[58] Moreover, at this alkaline pH, the organic material would become negatively charged species as deprotonation occurs (pK_a's in Table 1), which would lead to electrostatic repulsion onto the negatively charged mineral (PZC in Table 2). In experiments by Schwaminger et al., amino acid adsorption onto nanomagnetite particles is dependent on the side chain and point zero charge of the adsorbent; the negatively charged carboxyl functional group is likely the binding site on positively charged surfaces;[37] however, the functional groups in our organic acids may all be deprotonated leading to more negative surface charges.

Table 2. Surface Charge of Fe-Hydroxide Minerals and Fe-Sulfide Minerals

material	zero point charge (ZPC)	reference
green rust (sulfate and carbonate)	8.2	55
magnetite (Fe_3O_4)	6.5	56
hematite (Fe_2O_3)	8.6	56
FeS	3.3	57

Organic Acid Adsorption onto Fe-Sulfides. Previously reported density functional theory (DFT) adsorption studies of adsorption of methylamine onto the FeS mineral mackinawite observed adsorption on two surfaces of the material.[60] In density functional theory studies of the amino acid cysteine adsorbed onto FeS materials such as mackinawite, the functional groups of cysteine (e.g., thiol, amine, and carboxyl) were able to adsorb via H-bonding, van der Waals,

https://doi.org/10.1021/acsearthspacechem.4c00372
ACS Earth Space Chem. XXXX, XXX, XXX−XXX

and ligand exchange mechanisms.[61] While the mineral generated in the study likely is not pure mackinawite, these studies can contextualize what we are observing in our experiments.

Previous work has shown that functional groups of our organic material may also bind to mineral surface sites, for example, glycine was able to bind in modeled simulations but not in laboratory experiments.[62] In the same review, alanine and other amino acids were reported to weakly bind onto TiO_2 surfaces; alanine binds onto maghemite only by electrostatic interactions.[62] The organic materials we chose are negatively charged at a pH of 10, and previous work has shown the pH dependence on the binding of both mineral surfaces and organic molecules. Work by Lambert on glycine adsorption on silica surfaces suggests weak binding interactions.[52] However, for our minerals containing Fe, in several cases, the binding site and strength are directly related to the zero-point charge (ZPC) of the material. The ZPC of our materials is listed in Table 2 and shows that our mineral surfaces are negatively charged at a pH of 10 (Table 2). In addition to our experimental conditions having both a negatively charged mineral surface and negatively charged organic ion (negatively charged ions > pK_a/pK_2), our experiments may be further influenced by the solution's ionic strength.

In Fe-sulfide experiments, all the experiments beginning with any Fe^{3+} showed Fe reduction to Fe^{2+} (and experiments beginning with only Fe^{2+} remained reduced). Sulfide and Fe are both redox active; sulfide oxidizes into various species, potentially including elemental S or sulfate (SO_4^{2-}), while our Fe(III)-bearing minerals are reduced to ferrous precipitates.[53] Further, the conditions that simulated the Ceres brine contained additional species (dissolved $(NH_4)_2CO_3$, $NaHCO_3$, NH_4Cl, $MgCl_2{\bullet}6H_2O$, $NiCl_2$, $MgCO_3$, KCl) that increase the ionic strength. Our Ceres brine experiments have an increased ionic strength in comparison to our experiments without brine solution. The amount of Cl^- and Na^+ ions is at least 10 times the concentration of our amino acids in all of our experiments. Previous research has demonstrated that high ionic strength and pH play a critical role in decreasing adsorption.[58,62]

Since we observed that the organic material remains primarily in solution (and not bound to the Fe-hydroxide or sulfide minerals), the organics are mobile and available for reactivity. Other researchers have performed reactions with precursors, such as pyruvate, to the organic acids that were studied in the work presented here.[63,64] Possible organic chemistry on Ceres would be relevant for understanding what organic materials to expect and where they can be found on Ceres for future missions. Further understanding the organic inventory and its fate in the environment of Ceres is also important to understanding habitability.

CONCLUSIONS

Fe-hydroxides and Fe-sulfides may adsorb organic material, but this is highly dependent on the mineral structure, pH, and ionic strength of the solution under Ceres-relevant conditions. In our experiments, we observed negligible adsorption of organic material onto Fe-hydroxides and Fe-sulfides under alkaline conditions. This finding suggests that the organic material remained in the aqueous phase and may be easily transported in Fe-hydroxide- and Fe-sulfide-rich environments. While the alkaline pH of our experimental systems favors the precipitation of iron, it also would create minerals with negatively charged surfaces, which would repel the negatively charged organic molecules. In the presence of Ceres analogue brines, we observed little to no adsorption, even with dry/wetting cycles. This work could imply good sites for Ceres sample return concepts, as the organic material is indicated to be mobile under these conditions.

ASSOCIATED CONTENT

Supporting Information

The Supporting Information is available free of charge at https://pubs.acs.org/doi/10.1021/acsearthspacechem.4c00372.

Complete list of experimental conditions, reaction images, ^1H NMR spectra of the reaction time points, Ceres brine solution recipe, VNIR spectra, and colorimetry data (PDF)

AUTHOR INFORMATION

Corresponding Authors

Jessica M. Weber − *NASA Jet Propulsion Laboratory, California Institute of Technology, Pasadena, California 91109, United States;* orcid.org/0000-0002-8434-0066; Email: Jessica.weber@jpl.nasa.gov

Laura M. Barge − *NASA Jet Propulsion Laboratory, California Institute of Technology, Pasadena, California 91109, United States;* orcid.org/0000-0002-2187-540X; Email: laura.m.barge@jpl.nasa.gov

Authors

Eduardo Martinez − *NASA Jet Propulsion Laboratory, California Institute of Technology, Pasadena, California 91109, United States;* orcid.org/0009-0007-4222-0334

Erika Flores − *NASA Jet Propulsion Laboratory, California Institute of Technology, Pasadena, California 91109, United States;* orcid.org/0000-0003-0985-7564

Dennise Valadez − *NASA Jet Propulsion Laboratory, California Institute of Technology, Pasadena, California 91109, United States*

David VanderVelde − *Department of Chemistry, California Institute of Technology, Pasadena, California 91123, United States*

Rachel Y. Sheppard − *Planetary Science Institute, Tucson, Arizona 85719, United States; Institut d'Astrophysique Spatiale, Université Paris-Saclay, CNRS, Orsay 91440, France*

Robert Hodyss − *NASA Jet Propulsion Laboratory, California Institute of Technology, Pasadena, California 91109, United States*

Julie Castillo-Rogez − *NASA Jet Propulsion Laboratory, California Institute of Technology, Pasadena, California 91109, United States*

Mohit Melwani Daswani − *NASA Jet Propulsion Laboratory, California Institute of Technology, Pasadena, California 91109, United States;* orcid.org/0000-0002-4611-3209

Bryana L. Henderson − *NASA Jet Propulsion Laboratory, California Institute of Technology, Pasadena, California 91109, United States*

Complete contact information is available at: https://pubs.acs.org/10.1021/acsearthspacechem.4c00372

https://doi.org/10.1021/acsearthspacechem.4c00372
ACS Earth Space Chem. XXXX, XXX, XXX−XXX

Author Contributions

The manuscript was written through the contributions of all authors. All authors have given approval to the final version of the manuscript. E.M. contributed by writing the manuscript and performing experiments. E.F. and D.V. performed experiments. J.M.W. contributed by analyzing NMR. D.V. performed NMR. R.Y.S. performed VNIR. R.P.H., J.C.-R., M.M.D., and B.L.H. contributed to the editing of the manuscript. L.M.B. contributed by designing the experiments and interpreting the data. All authors contributed to the editing and/or writing of this work. All authors have approved the final version of this document.

Funding

This research was funded by a NASA JPL Strategic Research and Technology Development (R&TD) award "Fate of Organics on Ocean Worlds." This research was carried out at the Jet Propulsion Laboratory, California Institute of Technology, under a contract with NASA (80NM0018D004). Reference herein to any specific commercial product, process, or service by trade name, trademark, manufacturer, or otherwise does not constitute or imply its endorsement by the United States Government or the Jet Propulsion Laboratory, California Institute of Technology. Government sponsorship acknowledged. 2024. All rights reserved.

Notes

The authors declare no competing financial interest.

REFERENCES

(1) De Sanctis, M. C.; Ammannito, E.; McSween, H. Y.; Raponi, A.; Marchi, S.; Capaccioni, F.; Capria, M. T.; Carrozzo, F. G.; Ciarniello, M.; Fonte, S.; Formisano, M.; Frigeri, A.; Giardino, M.; Longobardo, A.; Magno, G.; McFadden, L. A.; Palomba, E.; Pieters, C. M.; Tosi, F.; Zambon, F.; Raymond, C. A.; Russell, C. Localized aliphatic organic material on the surface of Ceres. *Science* **2017**, *355*, 719−722.

(2) De Sanctis, M. C.; Mitri, G.; Castillo-Rogez, J.; House, C. H.; Marchi, S.; Raymond, C. A.; Sekine, Y. Relict Ocean Worlds: Ceres. *Space Sci. Rev.* **2020**, *216*, 1−33.

(3) Russell, C. T.; Raymond, C. A.; Ammannito, E.; Buczkowski, D. L.; De Sanctis, M. C.; Hiesinger, H.; Jaumann, R.; et al. Dawn arrives at Ceres: Exploration of a small, volatile-rich world. *Science* **2016**, *353*, 1008−1010.

(4) Castillo-Rogez, J.; Brophy, J.; Miller, K.; Sori, M.; Scully, J.; Quick, L.; Grimm, R.; Zolensky, M.; et al. Concepts for the future exploration of dwarf planet Ceres' habitability. *Planet Sci. J.* **2022**, *3*, 41.

(5) Castillo-Rogez, J. Future exploration of Ceres as an ocean world. *Nat. Astron.* **2020**, *4*, 732−734.

(6) National Academies of Sciences, Engineering, and Medicine. *Origins, worlds, and life: a decadal strategy for planetary science and astrobiology 2023−2032*. The National Academies Press: Washington DC, 2023.

(7) Castillo-Rogez, J. C.; Neveu, M.; Scully, J. E. C.; House, C. H.; Quick, L. C.; Bouquet, A.; Miller, K.; Bland, M.; et al. Ceres: astrobiological target and possible ocean world. *Astrobio.* **2020**, *20*, 269−291.

(8) Hendrix, A. R.; Hurford, T. A.; Barge, L. M.; Bland, M. T.; Bowman, J. S.; Brinckerhoff, W.; Buratti, B. J.; et al. The NASA roadmap to ocean worlds. *Astrobio.* **2019**, *19*, 1−27.

(9) Ammannito, E.; De Sanctis, M.; Ciarniello, M.; Frigeri, A.; Carrozzo, F. G.; Combe, J.-P.; Ehlmann, B.; Marchi, S.; McSween, H. Y.; Raponi, A.; et al. Distribution of phyllosilicates on the surface of Ceres. *Science* **2016**, *353*, No. aaf4279.

(10) De Sanctis, M. C.; Ammannito, E.; Raponi, A.; Marchi, S.; McCord, T. B.; McSween, H. Y.; Capaccioni, F.; Capria, M. T.; et al. Ammoniated phyllosilicates with a likely outer Solar System origin on (1) Ceres. *Nature* **2015**, *528*, 241−244.

(11) Marchi, S.; Raponi, A.; Prettyman, T. H.; De Sanctis, M. C.; Castillo-Rogez, J. C.; Raymond, C. A.; Ammannito, E.; Bowling, T.; Ciarniello, M.; et al. An aqueously altered carbon-rich Ceres. *Nat. Astron.* **2019**, *3*, 140−145.

(12) Castillo-Rogez, J. C.; Neveu, M.; McSween, H. Y.; Fu, R. R.; Toplis, M. J.; Prettyman, T. Insights into Ceres's evolution from surface composition. *Meteorit. Planet. Sci.* **2018**, *53*, 1820−1843.

(13) Marchi, S.; Raponi, A.; Prettyman, T. H.; De Sanctis, M. C.; Castillo-Rogez, J.; Raymond, C. A.; et al. An aqueously altered carbon-rich Ceres. *Nat. Astron.* **2019**, *3*, 140−145.

(14) Bowling, T. J.; Johnson, B. C.; Marchi, S.; De Sanctis, M. C.; Castillo-Rogez, J. C.; Raymond, C. A. An endogenic origin of cerean organics. *Earth Planet. Sci. Lett.* **2020**, *534*, No. 116069.

(15) McSween, H. Y., Jr.; Emery, J. P.; Rivkin, A. S.; Toplis, M. J.; Castillo-Rogez, J. C.; Prettyman, T. H.; De Sanctis, C. M.; Pieters, C. M.; Raymond, C. A.; Russell, C. T. Carbonaceous chondrites as analogs for the composition and alteration of Ceres. *Meteorit. Planet. Sci.* **2017**, *53*, 1793−1804.

(16) Flores, E.; Martinez, E.; Rodriguez, L. E.; Weber, J. M.; Khodayari, A.; VanderVelde, D. G.; Barge, L. M. Effects of amino acids on phosphate adsorption onto iron (oxy) hydroxide minerals under early earth conditions. *ACS Earth Space Chem.* **2021**, *5* (5), 1048−1057.

(17) Bhattacharyya, A.; Schmidt, M. P.; Stavitski, E.; Azimzadeh, B.; Martínez, C. E. Ligands representing important functional groups of natural organic matter facilitate Fe redox transformations and resulting binding environments. *Geochim. Cosmochim. Acta* **2019**, *251*, 157−175.

(18) Joshani, A.; Mirzaei, Y.; Barber, A.; Balind, K.; Gobeil, C.; Gélinas, Y. Organic matter preservation through complexation with iron minerals in two basins of a dimictic boreal lake with contrasting deep water redox regimes. *Sci. Total Environ.* **2024**, *925*, No. 171776.

(19) dos Santos, R.; Patel, M.; Cuadros, J.; Martins, Z. Influence of mineralogy on the preservation of amino acids under simulated Mars conditions. *Icarus* **2016**, *277*, 342−353.

(20) De Sanctis, M. C.; Raponi, A.; Ammannito, E.; Ciarniello, M.; Toplis, M. J.; McSween, H. Y.; Castillo-Rogez, J. C.; Elhmann, B. L.; Carrozzo, F. G.; Marchi, S.; Tosi, F.; Zambon, F.; Capaccioni, F.; Capria, M. T.; Fonte, S.; Formisano, M.; Frigeri, A.; Giardino, M.; Longobardo, A.; Magni, G.; Palomba, E.; McFadden, L. A.; Pieters, C. M.; Jaumann, R.; Schenk, P.; Mugnuolo, R.; Raymond, C. A.; Russell, C. T. Bright carbonate deposits as evidence of aqueous alteration on (1) Ceres. *Nature* **2016**, *536* (7614), 54−57.

(21) Durmus, Z.; Kavas, H.; Toprak, M. S.; Baykal, A.; Altınçekiç, T. G.; Aslan, A.; Bozkurt, A.; Coşgun, S. L-lysine coated iron oxide nanoparticles: synthesis, structural and conductivity characterization. *J. Alloys Compd.* **2009**, *484*, 371−376.

(22) Pušnik, K.; Peterlin, M.; Cigić, I. K.; Marolt, G.; Kogej, K.; Mertelj, A.; Gyergyek, S.; Makovec, D. Adsorption of amino acids, aspartic acid, and lysine onto iron-oxide nanoparticles. *J. Phys. Chem. C* **2016**, *120*, 14372−14381.

(23) De Sanctis, M. C.; Vinogradoff, V.; Raponi, A.; Ammannito, E.; Ciarniello, M.; Carrozzo, F. G.; De Angelis, S.; Raymond, C. A.; Russell, C. T. Characteristics of organic matter on Ceres from VIR/Dawn high spatial resolution spectra. *Mon. Not. R. Astron. Soc.* **2019**, *482*, 2407−2421.

(24) Vinogradoff, V.; Poggiali, G.; Raponi, A.; Ciarniello, M.; De Angelis, S.; Ferrari, M.; Castillo-Rogez, J. C.; Brucato, J.; De Sanctis, M. C. Laboratory investigations coupled to VIR/Dawn observations to quantify the large concentrations of organic matter on Ceres. *Minerals.* **2021**, *11*, 719.

(25) Hoehler, T.; Bains, W.; Davila, A.; Parenteau, M.; Pohorille, A. Life's requirements, habitability, and biological potential. *Planet. Astrobiol.* **2020**, *13*, 37.

(26) Eschenmoser, A. The search for the chemistry of life's origin. *Tetrahedron* **2007**, *63* (52), 12821−12844.

https://doi.org/10.1021/acsearthspacechem.4c00372
ACS Earth Space Chem. XXXX, XXX, XXX−XXX

(27) Williamson, M. P. Autocatalytic Selection as a Driver for the Origin of Life. *Life* **2024**, *14* (5), 590.
(28) Miller, S. L. The mechanism of synthesis of amino acids by electric discharges. *Biochim. Biophys. Acta* **1957**, *23*, 480−489.
(29) Barge, L. M.; Flores, E.; Baum, M. M.; VanderVelde, D. G.; Russell, M. J. Redox and pH gradients drive amino acid synthesis in iron oxyhydroxide mineral systems. *Proc. Natl. Acad. Sci. U.S.A.* **2019**, *116*, 4828−4833.
(30) Koga, T.; Naraoka, H. Synthesis of amino acids from aldehydes and ammonia: Implications for organic reactions in carbonaceous chondrite parent bodies. *Earth Space Chem.* **2022**, *6*, 1311−1320.
(31) Otake, T.; Wesolowski, D. J.; Anovitz, L. M.; Allard, L. F.; Ohmoto, H. Mechanisms of iron oxide transformations in hydrothermal systems. *Geochim. Cosmochim. Acta* **2010**, *74* (21), 6141−6156.
(32) Peiffer, S.; Behrends, T.; Hellige, K.; Larese-Casanova, P.; Wan, M.; Pollok, K. Pyrite formation and mineral transformation pathways upon sulfidation of ferric hydroxides depend on mineral type and sulfide concentration. *Chem. Geol.* **2015**, *400*, 44−55.
(33) Barge, L. M.; Flores, E.; Weber, J. M.; Fraeman, A. A.; Yung, Y. L.; VanderVelde, D.; Martinez, E.; Castonguay, A.; Billings, K.; Baum, M. M. Prebiotic reactions in a Mars analog iron mineral system: effects of nitrate, nitrite, and ammonia on amino acid formation. *Geochim. Cosmochim. Acta* **2022**, *336* (336), 469−479.
(34) Novikov, Y.; Copley, S. D. Reactivity landscape of pyruvate under simulated hydrothermal vent conditions. *Proc. Natl. Acad. Sci. U.S.A.* **2013**, *110*, 13283−13288.
(35) Huber, C.; Wächtershäuser, G. α-Hydroxy and α-amino acids under possible Hadean, volcanic origin-of-life conditions. *Science* **2006**, *314* (314), 630−632.
(36) Aguirre, V. P.; Jocic, S.; Webster, P.; Buser, C.; Moss, J. A.; Barge, L. M.; Tang, Y.; Guo, Y.; Baum, M. M. Synthesis and characterization of mixed-valent iron layered double hydroxides ("green rust"). *Earth Space Chem.* **2021**, *5*, 40−54.
(37) Schwaminger, S. P.; García, P. F.; Merck, G. K.; Bodensteiner, F. A.; Heissler, S.; Günther, S.; Berensmeier, S. Nature of interactions of amino acids with bare magnetite nanoparticles. *J. Phys. Chem. C* **2015**, *119*, 23032−23041.
(38) Locke, M. J.; McIver, R. T., Jr Effect of solvation on the acid/base properties of glycine. *J. Am. Chem. Soc.* **1983**, *105*, 4226−4232.
(39) Reisinger, H.; King, C. J. Extraction and sorption of acetic acid at pH above pKa to form calcium magnesium acetate. *Ind. Eng. Chem. Res.* **1995**, *34*, 845−852.
(40) Max, J. J.; Chapados, C. Infrared spectroscopy of aqueous carboxylic acids: malic acid. *J. Phys. Chem. A* **2002**, *106*, 6452−6461.
(41) Urry, D. W.; Gowda, D. C.; Peng, S.; Parker, T. M.; Jing, N.; Harris, R. D. Nanometric design of extraordinary hydrophobic-induced pKa shifts for aspartic acid: Relevance to protein mechanisms. *Biopolymers: Original Research on Biomolecules.* **1994**, *34*, 889−896.
(42) Clark, R. N.; Roush, T. L. Reflectance spectroscopy: Quantitative analysis techniques for remote sensing applications. *J. Geophys. Res: Solid Earth.* **1984**, *89*, 6329−6340.
(43) Bishop, J. L.; Pieters, C.; Burns, R. G. Reflectance and Mössbauer spectroscopy of ferrihydrite-montmorillonite assemblages as Mars soil analog materials. *Geochim. Cosmochim. Acta* **1993**, *57*, 4583−4595.
(44) Horgan, B. H.; Cloutis, E. A.; Mann, P.; Bell, J. F., III Near-infrared spectra of ferrous mineral mixtures and methods for their identification in planetary surface spectra. *Icarus.* **2014**, *234*, 132−154.
(45) Viviano, C. E.; Seelos, F. P.; Murchie, S. L.; Kahn, E. G.; Seelos, K. D.; Taylor, H. W.; Taylor, K.; et al. Revised CRISM spectral parameters and summary products based on the currently detected mineral diversity on Mars. *J. of Geophys. Res.: Planets.* **2014**, *119*, 1403−1431.
(46) Milliken, R. RELAB spectral library bundle. *NASA Planet. Data Syst.* **2020**, 98.
(47) Sklute, E. C.; Jensen, H. B.; Rogers, A. D.; Reeder, R. J. Morphological, structural, and spectral characteristics of amorphous iron sulfates. *J. Geophys. Res.: Planets* **2015**, *120*, 809−830.
(48) Sklute, E. C.; Kashyap, S.; Dyar, M. D.; Holden, J. F.; Tague, T.; Wang, P.; Jaret, S. J. Spectral and morphological characteristics of synthetic nanophase iron (oxyhydr)oxides. *Phys. Chem. Miner.* **2018**, *45* (1), 1−26.
(49) Sheppard, R. Y.; Milliken, R. E.; Russell, J. M.; Dyar, M. D.; Sklute, E. C.; Vogel, H.; Melles, M.; et al. Characterization of iron in Lake Towuti sediment. *Chem. Geol.* **2019**, *512*, 11−30.
(50) Izawa, M. R.; Cloutis, E. A.; Rhind, T.; Mertzman, S. A.; Applin, D. M.; Stromberg, J. M.; Sherman, D. M. Spectral reflectance properties of magnetites: Implications for remote sensing. *Icarus.* **2019**, *319*, 525−539.
(51) Matrajt, G.; Blanot, D. Properties of synthetic ferrihydrite as an amino acid adsorbent and a promoter of peptide bond formation. *Amino acids.* **2004**, *26*, 153−158.
(52) Lambert, J. F. Adsorption and polymerization of amino acids on mineral surfaces: a review. *Orig. Life Evol. Biosph.* **2008**, *38*, 211−242.
(53) Firer, D.; Friedler, E.; Lahav, O. Control of sulfide in sewer systems by dosage of iron salts: comparison between theoretical and experimental results, and practical implications. *Sci. Total Environ.* **2008**, *392*, 145−156.
(54) Jonsson, C. M.; Jonsson, C. L.; Estrada, C.; Sverjensky, D. A.; Cleaves, H. J., II; Hazen, R. M. Adsorption of l-aspartate to rutile (α-TiO2): experimental and theoretical surface complexation studies. *Geochim. Cosmochim. Acta* **2010**, *74*, 2356−2367.
(55) Guilbaud, R.; White, M. L.; Poulton, S. W. Surface charge and growth of sulphate and carbonate green rust in aqueous media. *Geochim. Cosmochim. Acta* **2013**, *108*, 141−153.
(56) Xu, Y.; Schoonen, M. A. The absolute energy positions of conduction and valence bands of selected semiconducting minerals. *Am. Mineral.* **2000**, *85* (3−4), 543−556.
(57) Bebie, J.; Schoonen, M. A. A.; Fuhrmann, M.; Strongin, D. R. Surface charge development on transition metal sulfides: an electrokinetic study. *Geochim. Cosmochim. Acta* **1998**, *62*, 633−642.
(58) Gao, Q.; Xu, W.; Xu, Y.; Wu, D.; Sun, Y.; Deng, F.; Shen, W. Amino acid adsorption on mesoporous materials: influence of types of amino acids, modification of mesoporous materials, and solution conditions. *J. Phys. Chem. B* **2008**, *112*, 2261−2267.
(59) Filius, J. D.; Hiemstra, T.; Van Riemsdijk, W. H. Adsorption of small weak organic acids on goethite: Modeling of mechanisms. *J. Colloid Interface Sci.* **1997**, *195*, 368−380.
(60) Dzade, N. Y.; Roldan, A.; De Leeuw, N. H. Adsorption of methylamine on mackinawite (FeS) surfaces: A density functional theory study. *J. Chem. Phys.* **2013**, *139*, No. 124708.
(61) Dzade, N. Y.; Roldan, A.; de Leeuw, N. H. Surface and shape modification of mackinawite (FeS) nanocrystals by cysteine adsorption: a first-principles DFT-D2 study. *Phys. Chem. Chem. Phys.* **2016**, *18*, 32007−32020.
(62) Costa, D.; Savio, L.; Pradier, C. M. Adsorption of amino acids and peptides on metal and oxide surfaces in water environment: a synthetic and prospective review. *J. Phys. Chem. B* **2016**, *120*, 7039−7052.
(63) Vu, T. H.; Reynoso, L. R.; Johnson, P. V.; Hodyss, R. Amino Acid-Mediated Formation of CO2 in Flash-Frozen Ceres Brines. *Earth Space Chem.* **2024**, *8*, 1214−1223.
(64) Weber, J. M.; Czaplinski, E. C.; Henderson, B. L.; Barge, L. M.; Castillo-Rogez, J. C.; Hodyss, R. Photochemical Stability and Reactivity of Sodium Pyruvate: Implications for Organic Analysis on Ceres. *ACS Earth Space Chem.* **2024**, *8*, 1385−1393.

https://doi.org/10.1021/acsearthspacechem.4c00372
ACS Earth Space Chem. XXXX, XXX, XXX−XXX